



Research article

The new challenge of partial oxidation of methane over Fe₂O₃/NaY and Fe₃O₄/NaY heterogeneous catalystsY.K. Krisnandi^{a,b,*}, D.A. Nurani^{a,b}, D.V. Alfian^a, U. Sofyani^{a,b}, M. Faisal^a, I.R. Saragi^{b,c}, A.Z. Pamungkas^{a,b}, A.P. Pratama^{a,b}^a Department of Chemistry, Faculty of Mathematics and Natural Science, Universitas Indonesia, Depok-16424, Indonesia^b Solid Inorganic Framework Laboratory, Department of Chemistry, Faculty of Mathematics and Natural Science, Universitas Indonesia, Depok-16424, Indonesia^c Department of Chemistry, Faculty of Mathematics and Natural Science, Universitas Sumatera Utara, Medan-20155, Indonesia

ARTICLE INFO

Keywords:

NaY zeolite

Partial oxidation of methane

Methanol

Iron oxide

Heterogeneous catalyst

ABSTRACT

As one of the most important gases that abundantly contribute to air pollution, methane becomes the most leading gas that challenges researchers to utilize it in more functional products such as methanol. In this study, the conversion process involved iron oxide species supported by sodium Y (NaY-Z) zeolite as the catalysts. This work highlighted the preparation of Fe₂O₃ and Fe₃O₄ modified NaY zeolite to investigate their catalytic performance on partial oxidation of methane to methanol, with trace amount of oxygen (0.5% in N₂), in a batch reactor. The as-prepared catalysts were characterized using FTIR, XRD, SEM, and BET. The structure of NaY zeolite and its modified catalysts were confirmed. The pristine NaY-Z shows the highest activity followed by Fe₂O₃/NaY-3.52 (3.52 wt% of Fe loading) with high selectivity to formaldehyde (80%). Very high selectivity (~100%) towards methanol was observed in the reactions on Fe₂O₃/NaY-1.70 and Fe₃O₄/NaY-2.55 catalysts, although the total amount of product was decreased. It was noticeable that Fe₃O₄/NaY-3.22 is an active catalyst and has good selectivity to methanol (70%).

1. Introduction

Methane is the major component of natural gas followed by other longer chained alkanes such as butane and propane. It can also be found at the waste landfill or manure feedstock [1]. In addition, methane has great potential as a greenhouse gas [2]. Methane is usually used directly as fuel [3], especially in rural and agriculture areas. On the other hand, it also has potential as a raw material that can be converted into other valuable chemicals. However, its utilization can face some obstacles including transportation, in which it must be compressed at 10–100 atm due to its low density [4]. Therefore, it is highly desirable to convert methane, e.g. through direct catalytic reaction, to easily transported compounds such as methanol, acetic acid, formaldehyde, or aromatics [5].

Recent research activities on the direct catalytic conversion of methane are focused on its product selectivity. The challenge regarding the reaction selectivity that remains unresolved is that the catalyst has to overcome the stability of the C–H bond from CH₄ and the probability of over oxidation of CH₄ to CO₂ and H₂O, in which many catalysts have been explored [6, 7, 8, 9].

The first challenge is correlated to the activation process of C–H from the CH₄. Methane is a very stable non-polar molecule that is difficult to activate [10]. The second unresolved problem is correlated to the possibility of over oxidation of CH₄, which nowadays could be solved by generating active oxygen species that are also sufficiently reactive to activate the C–H bond of CH₄ [8]. Sharma et al [11] has reported significant results in the conversion of methane to methanol using methane monooxygenases that generate active oxygen species, abstracting C–H from methane. Rosa et al [12] reported a catalytic oxidation model using Fe/ZSM-5 as the catalyst and molecular oxygen as oxidizing agent. The active oxygen species was labeled as α-oxygen, which is the anion radical species O⁻ associated with trivalent iron in the Fe/ZSM-5 zeolite matrix. The reaction was conducted at a relatively mild temperature of about 433 K, leading directly to methanol production, accumulated on the Fe/ZSM-5 surface [12].

Starokon et al [13] performed the catalytic oxidation of CH₄ using Fe/ZSM-5 zeolite with pre-deposited α-oxygen. In this work, the α-oxygen was formed during N₂O decomposition at 423–473 K on α sites (Fe^{II})_α. The room temperature reaction of methane with α-oxygen

* Corresponding author.

E-mail address: yuni.krisnandi@sci.ui.ac.id (Y.K. Krisnandi).

generated the abstraction of a hydrogen atom that led to the formation of hydroxy and methoxy groups residing on α -sites [13]. The results showed that the CH_3^\bullet abstracted from CH_4 , caused by the reaction of $(\text{O})_\alpha$ species and one hydrogen atom, underwent further reaction with methoxy groups at the surface of Fe/ZSM-5 zeolite to form dimethyl ether and it also bound to zeolites which then upon heating were oxidized to CO_x . This over-oxidation problem has been resolved in another study by Starokon et al [14].

Bitter et al [15] initiated the research in partial oxidation of methane to methanol and formaldehyde over Co/ZSM-5 molecular sieve. Our previous work has adapted their work and modified it by comparing micro with hierarchical ZSM-5 as catalysts, varying the methods to prepare Co/ZSM-5, and performing reactions with or without trace amounts of O_2 as oxidation agent [16, 17, 18]. It showed that Co_3O_4 impregnated on hierarchical ZSM-5 zeolite was the best catalyst with the highest methanol yield (42 %) and a very small amount of formaldehyde [16]. Further work has been carried out to replace the cobalt oxide (Co_3O_4) with other metal oxides such as NiO, Mn_3O_4 , and Fe_2O_3 [19, 20]. It has shown that iron oxide species (Fe_2O_3) is the best candidate to replace cobalt oxide providing a 30% yield of methanol while other catalysts are less active.

Research on the partial oxidation of methane using ZSM-5 zeolite supports obtained from natural resources, such as coal fly ash and rice husk, has also been reported [21]. However, all of those reactions have poor selectivity. The resulting products varied from methanol, formaldehyde, and formic acid. Since the synthesis of ZSM-5 zeolite requires the expensive TPAOH as an organic template and several days of crystallization, using another type of zeolite that is more feasible in synthesis becomes a challenge. Thus, NaY with faujasite (FAU) structure was taken into account. NaY zeolite has Si/Al ratio between 2-4, large pore opening and cavity, surface area, adsorption capacity, good thermal stability, and active sites with diverse strength [21], and most importantly it is more feasible to prepare compared to ZSM-5 zeolites. Therefore, in this work, the reaction was carried out using NaY zeolite impregnated with Fe_2O_3 or Fe_3O_4 to observe the reaction selectivity towards methanol.

2. Materials and methods

2.1. Materials

Sodium aluminate (NaAlO_2), colloidal silica (LUDOX HS-40), $\text{Fe}(\text{NO}_3)_3 \cdot 9\text{H}_2\text{O}$, $\text{FeCl}_2 \cdot 4\text{H}_2\text{O}$, $\text{FeCl}_3 \cdot 6\text{H}_2\text{O}$, sodium hydroxide (NaOH), and ammonium hydroxide (NH_4OH) were purchased from Sigma Aldrich, methane gas 99.9% (BOC), nitrogen gas 99.99% UHP and mixed gas of 0.5% oxygen in 99.5% nitrogen were supplied by CV Retno Gas (Jakarta).

2.2. Catalyst preparation

2.2.1. Synthesis of NaY zeolite

NaY zeolite was synthesized by adopting the previous reported method [22] typically by mixing NaAlO_2 , colloidal silica (LUDOX HS-40), NaOH, and distilled water with a molar ratio of 4.3 Na_2O : Al_2O_3 : 10 SiO_2 : 180 H_2O . The mixture was vigorously stirred for 3 h before

placed into a 200 mL Teflon-lined stainless-steel autoclave for the hydrothermal process at 373 K for 24 h. Then the white precipitate was filtered, and calcined at 373 K. The as-synthesized zeolite was labeled NaY-Z.

2.2.2. $\text{Fe}_2\text{O}_3/\text{NaY}$ preparation

Impregnation of Fe_2O_3 on NaY was conducted as follows. About 1 g of NaY zeolite was added to iron (III) solution (0.0626 M) from $\text{Fe}(\text{NO}_3)_3 \cdot 9\text{H}_2\text{O}$ and stirred for 24 h at room temperature until all surface water evaporated. To obtain $\text{Fe}_2\text{O}_3/\text{NaY}$, the precipitate was calcined at 823 K for 5.5 h. The two as-prepared $\text{Fe}_2\text{O}_3/\text{NaY}$ were labeled as $\text{Fe}_2\text{O}_3/\text{NaY-x}$ where x was wt% of Fe in the catalyst obtained from XRF measurement.

2.2.3. Fe_3O_4 and $\text{Fe}_3\text{O}_4/\text{NaY}$ preparation

Fe_3O_4 was synthesized using a co-precipitation method adopted from the previous method [23]. Fe (II) and Fe (III) solution from FeCl_2 and FeCl_3 , respectively was mixed with a molar ratio of 1:2 then the base solution (NH_4OH 1 M) was added dropwise to the mixture, and stirred for 24 h to obtain homogeneous Fe_3O_4 suspension. To obtain Fe_3O_4 catalyst, the black powder was separated from the suspension by decantation method, then washed and dried at 373 K. $\text{Fe}_3\text{O}_4/\text{NaY}$ was prepared by mixing a certain amount of the Fe_3O_4 suspension into 1 g of NaY zeolite. The mixture was stirred for 6 h at room temperature. Then the obtained powder was filtered, washed, and dried at 373 K for 2 h. The two as-prepared $\text{Fe}_3\text{O}_4/\text{NaY}$ were labeled as $\text{Fe}_3\text{O}_4/\text{NaY-y}$ where y was wt% of Fe in the catalyst obtained from XRF measurement.

2.3. Characterization of samples

The powder result was characterized using PANalytical: X'Pert Pro XRD diffractometer with Cu-K radiation ($\lambda = 1.54184 \text{ \AA}$) as the incident beam, Epsilon1 X-Ray Fluorescence Spectrometer (XRF) Elemental analysis, Alpha Bruker FTIR spectrometer, Quantachrome Surface Area Analyzer for complete surface area analysis, and SEM-EDS mapping for morphology of the catalysts. Surface area of catalysts was analyzed on a Surface Area Analyzer (SAA) Quantachrom-Evo Surface Area and Pore Analyzer at 77 K. SEM-EDS mapping was carried out on Scanning Electron Microscope (SEM) Quanta 650 operated at an accelerating voltage 2 kV.

2.4. Catalytic test: partial oxidation of methane

The catalytic test on partial oxidation of methane was carried out using the previous procedure [17]. The tested catalysts were NaY-Z, Fe_2O_3 /and Fe_3O_4 /modified NaY-Z catalysts, and Fe_3O_4 solid (c.a. 0.5 g). Prior to use, the catalysts were activated at 823K flushed with flowing nitrogen gas. The reaction condition was fixed to CH_4 : N_2 (0.5% O_2) ratio of 0.75: 2 (in atm), at 423 K, and a reaction time of 120 min. After cooling down to room temperature, the product was extracted from the catalysts using 2 mL of ethanol and directly analyzed using gas chromatography with a carbowax column and flame ionization detector (GC FID, Shimadzu 2010). The calculation on total amount of product and % selectivity is available in S1.

Table 1. XRF and Surface area analysis data for all catalysts.

Catalyst	XRF		Surface area analysis						
	Si/Al	Fe	S_{BET} (m^2/g)	S_{micro} (m^2/g)	S_{ext} (m^2/g)	V_{total} (cc/g)	V_{micro} (cc/g)	V_{ext} (cc/g)	Av. pore diameter (nm)
NaY-Z	4.20	0.06	382	370	12	0.22	0.21	0.01	3.80
$\text{Fe}_2\text{O}_3/\text{NaY-1.7}$	4.03	1.70	360	355	5	0.21	0.20	0.01	3.80
$\text{Fe}_2\text{O}_3/\text{NaY-3.52}$	3.78	3.52	500	457	43	0.29	0.26	0.03	3.80
$\text{Fe}_3\text{O}_4/\text{NaY-2.55}$	3.70	2.52	448	404	44	0.26	0.23	0.03	3.80
$\text{Fe}_3\text{O}_4/\text{NaY-3.22}$	3.64	3.22	473	446	27	0.28	0.25	0.03	3.80

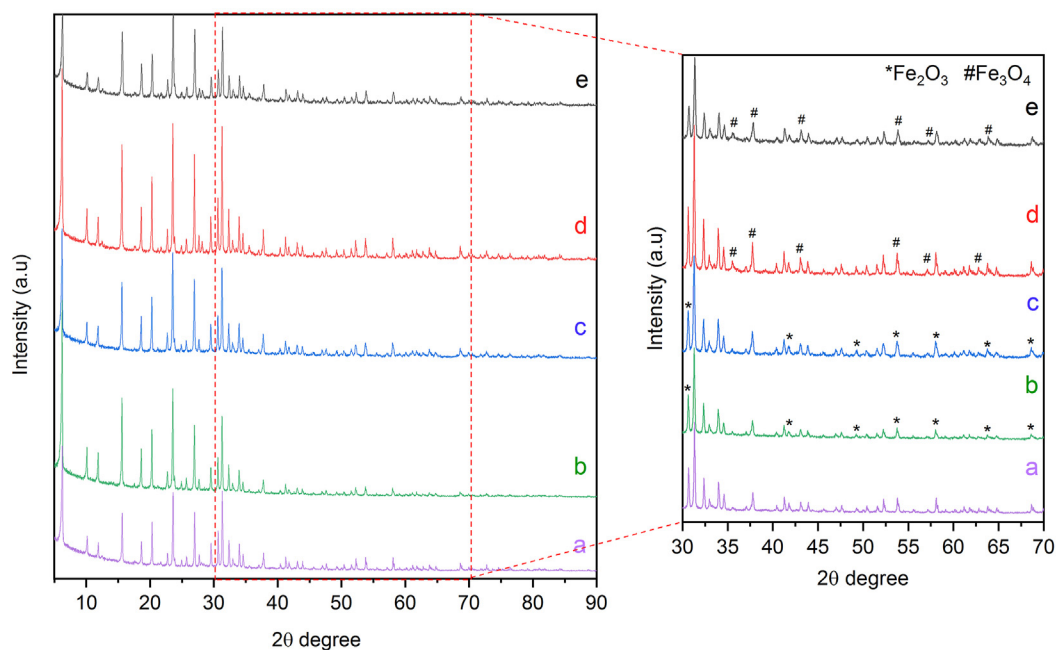


Figure 1. Powder XRD patterns of a) NaY-Z, b) $\text{Fe}_2\text{O}_3/\text{NaY}$ -1.7, c) $\text{Fe}_2\text{O}_3/\text{NaY}$ -3.52, d) $\text{Fe}_3\text{O}_4/\text{NaY}$ -2.55 and e) $\text{Fe}_3\text{O}_4/\text{NaY}$ -3.22.

3. Result

3.1. Catalyst characterization

3.1.1. XRF measurement

Synthesis of NaY Zeolite was performed by low-cost synthesis approach using a certain amount of colloidal silica (LUDOX HS-40), sodium aluminate (NaAlO_2) as silica and alumina source, respectively, without using structure directing agent or organic template [22]. The as-synthesized NaY (labeled as NaY-Z) was then modified with a certain

amount of Fe_2O_3 or Fe_3O_4 . The $\text{Fe}_3\text{O}_4/\text{NaY}$ -2.55 and $\text{Fe}_3\text{O}_4/\text{NaY}$ -3.22 catalysts were attracted by magnet (available in S2, Figure S1), indicative of the existence of magnetic Fe_3O_4 .

The XRF measurement provides information on Si/Al ratio and the elemental compositions of Fe in NaY zeolite after impregnation (available in S3, Table S1) which is summarized in Table 1, while the Na content of the catalysts was constant at 10.1–10.8 before and after modification (available in S3, Table S2). The Si/Al ratio in iron oxide modified NaY-Z tends to decrease, especially in higher Fe loading due to desilication during the modification process. Initially, the Si/Al ratio of

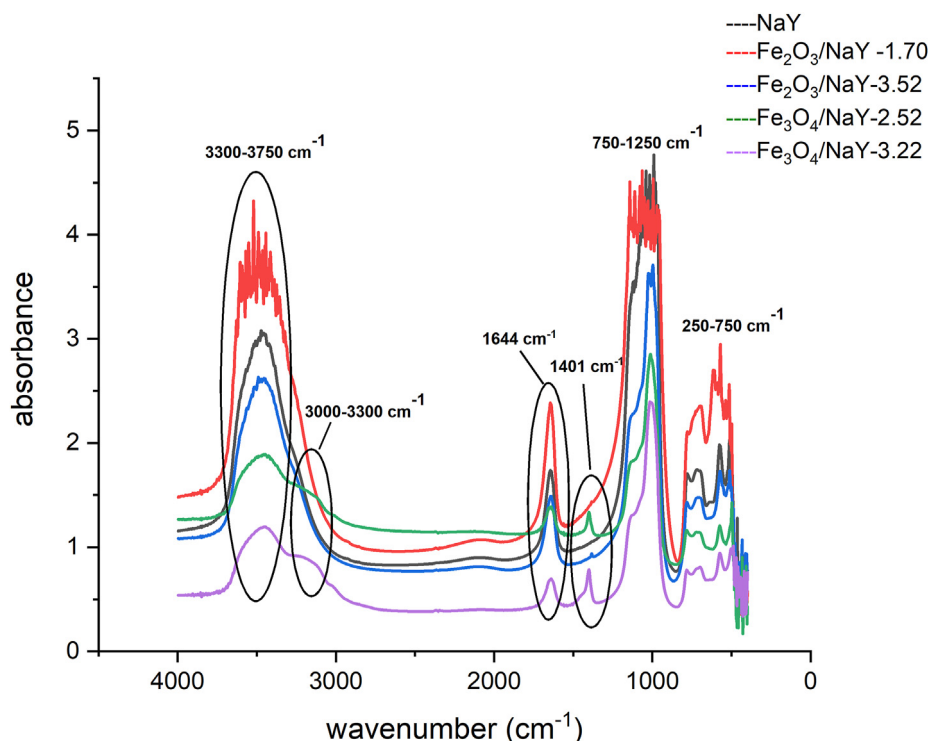


Figure 2. FTIR spectra of as-synthesized NaY and Fe_2O_3 - and Fe_3O_4 -modified NaY.

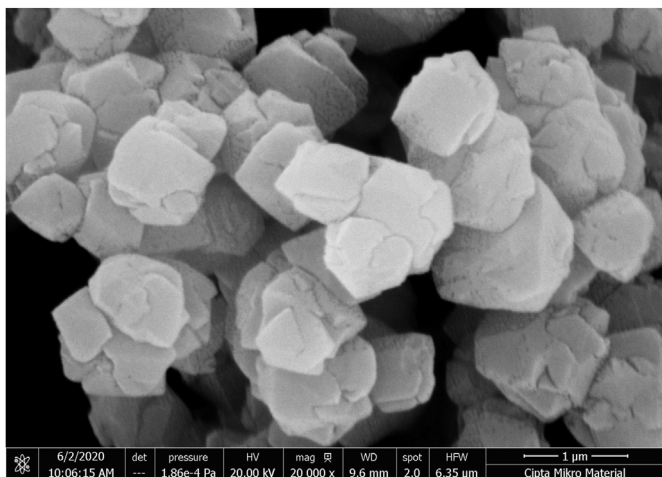


Figure 3. SEM images of as-synthesized NaY at a magnification of 20000 \times .

NaY-Z was 4.20, and slightly decreased after being impregnated with Fe_2O_3 (4.03–3.78). The pH of NaY and Fe^{3+} solution mixture was decreased to 5–6 during Fe_2O_3 impregnation, which give small impact to the NaY framework stability. On the other hand, the pH of the mixture during preparation of $\text{Fe}_3\text{O}_4/\text{NaY}$ was deliberately fixed to 11, so desilication (Si removal) may occur so the Si/Al decreased to 3.70–3.64.

3.1.2. Analysis of X-Ray diffraction (XRD)

The structural characterization was carried out using XRD. Powder XRD pattern of as-synthesized zeolite, NaY-Z (Figure 1) confirms the structure of Y zeolite with faujasite framework, where peaks at $2\theta = 6^\circ, 10^\circ, 11^\circ, 16^\circ, 19^\circ, 20^\circ, 24^\circ, 27^\circ,$ and 31° are observed [24]. Meanwhile, the XRD pattern of $\text{Fe}_2\text{O}_3/\text{NaY}$ zeolite shows an additional peak at $2\theta = 30^\circ, 42^\circ,$ and 64° ; according to JCPDS: 33-0664, the peaks belong to Fe_2O_3 lattice planes [25]. These results indicate the successful preparation of $\text{Fe}_2\text{O}_3/\text{Na-Y}$ zeolite. On the other hand, additional peaks at $2\theta = 42-44^\circ$ and $62-64^\circ$ are observed at the XRD pattern of $\text{Fe}_3\text{O}_4/\text{Na-Y}$ zeolite; according to JCPDS: 75-0033, the peaks belong to Fe_3O_4 crystals [26]. These results also indicate that the impregnation of Fe_3O_4 into the Na-Y zeolite surface was accomplished.

3.1.3. Analysis of Fourier transform InfraRed (FTIR)

Figure 2 shows the FTIR spectra of as-synthesized NaY before and after iron-oxide modification. The characteristic spectra for both materials are almost identical which is in accordance with the zeolitic framework. However, in $\text{Fe}_3\text{O}_4/\text{NaY}$, the intensity of the broadband in the range of $3300-3750\text{ cm}^{-1}$, assigned to the stretching vibration of water-hydrogen bonded silanol groups or internal silanol groups [27], decreases. This is due to the presence of iron oxide in the vicinity of the

silanol group that has hindered the interaction between water molecules and the silanol group. It is also observed in infrared spectra of $\text{Mn}_3\text{O}_4/\text{ZSM-5}$ [28]. The existence of magnetic phase iron oxides is indicated by the appearance of the peaks observed at 1401 cm^{-1} and 626 cm^{-1} in $\text{Fe}_3\text{O}_4/\text{NaY-2.55}$ and $\text{Fe}_3\text{O}_4/\text{NaY-3.22}$ were assigned to Fe-O bending and Fe-O stretching vibration, respectively [29].

3.1.4. Analysis of scanning electron microscopy (SEM)

The SEM image in Figure 3 shows the morphology of the as-synthesized NaY zeolite that exhibits sharp-edged cuboid-octahedral crystal habits, which is the characteristic of NaY zeolite [30, 31, 32]. It also has smooth surfaces, indicative of high crystalline as also supported by the well-defined XRD pattern. The crystal size is homogeneous, approximately $\sim 1\ \mu\text{m}$.

Figure 4 shows the morphology of $\text{Fe}_2\text{O}_3/\text{NaY}$ zeolites. It can be seen that the surface of NaY zeolites gradually becomes rougher when the amount of Fe_2O_3 increases (Figure 4a-b). This occurs due to change in pH of zeolite suspension from 8 to 6 during exposure to iron (III) in incipient wetness. From XRF measurement, the Si/Al ratio after the impregnation was slightly decreased $\text{Fe}_2\text{O}_3/\text{NaY-1.70}$ and became lower at $\text{Fe}_2\text{O}_3/\text{NaY-3.52}$. The presence of Fe_2O_3 anchoring to the surface of the NaY crystals also contributes to the change in the morphology of the zeolite crystals.

Similar to $\text{Fe}_2\text{O}_3/\text{NaY}$, the Fe_3O_4 impregnation treatment on NaY zeolite has caused the morphological surface of zeolite NaY to be rougher when compared to NaY zeolite before impregnation treatment (Figure 5a-b). This occurs due to desilication or removal of silicates during impregnation process with Fe^{3+} solution that caused the pH of zeolite increased from 8 to 11.

3.1.5. Analysis of surface area analysis (SAA)

From the adsorption-desorption isotherm graphs (Figure 6), it can be seen that both pristine and iron oxide modified NaY zeolites have type 1 isotherm curves which indicate that they are classified as microporous materials [33]. It can be seen that modification with iron-oxides through the impregnation method generates different effects on the surface area of the catalysts. It has caused the increase in the specific surface area of three iron oxide/NaY catalysts ($\text{Fe}_2\text{O}_3/\text{NaY-3.52}$, $\text{Fe}_3\text{O}_4/\text{NaY-2.55}$, and $\text{Fe}_3\text{O}_4/\text{NaY-3.22}$) in which the $\text{Fe}_2\text{O}_3/\text{NaY-3.52}$ catalyst has the highest specific surface area, $500\text{ m}^2/\text{g}$. This supports the observation with SEM showing that the iron oxides mostly impregnate the outer surfaces and create clusters and porosity [34]. The $\text{Fe}_2\text{O}_3/\text{NaY-1.70}$, On the other hand, experiences a decrease in specific surface area ($360\text{ m}^2/\text{g}$) compared to that of parent NaY, $382\text{ m}^2/\text{g}$, indicating that some iron oxides may reside inside the pores of the zeolite [35]. However, in other catalysts, after impregnation, the surface area increases due to the aggregation of Fe_2O_3 and Fe_3O_4 clusters on the NaY zeolite surface, creating more pores and volume. This was also observed by Wang et al when preparing iron oxide modified MCM-41 [36]. Summary of the result on surface area analysis has been tabulated in Table 1.

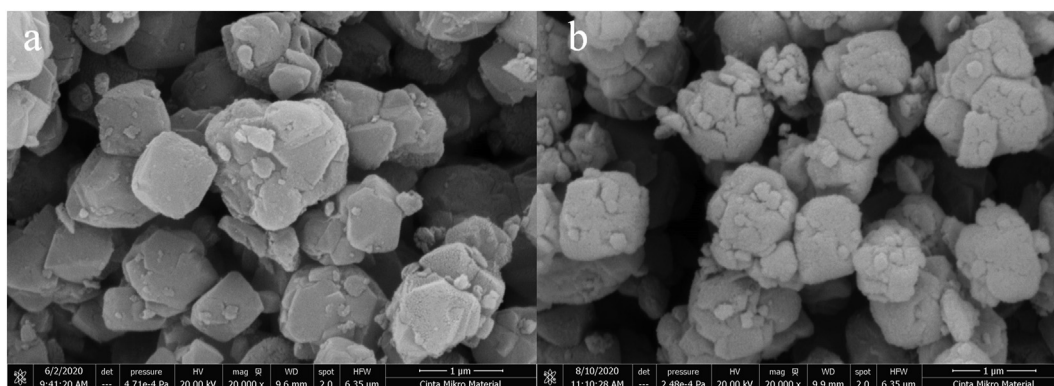


Figure 4. SEM images of (a) $\text{Fe}_2\text{O}_3/\text{NaY-1.3}$ and (b) $\text{Fe}_2\text{O}_3/\text{NaY-2.7}$ at magnification of 20000 \times .

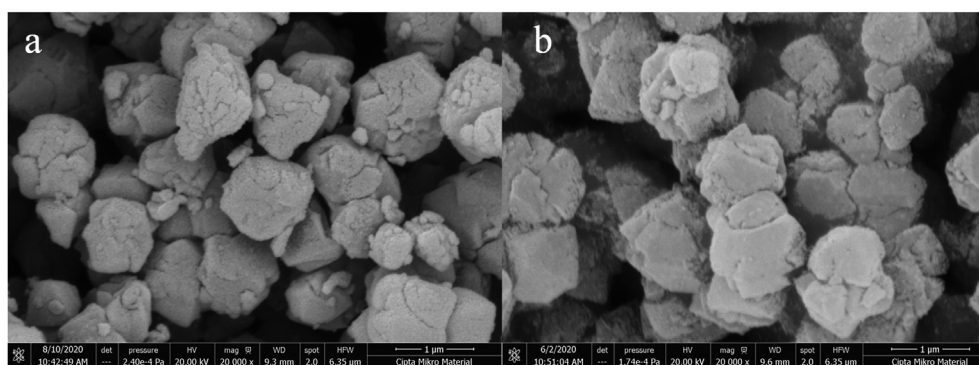


Figure 5. SEM images of (a) $\text{Fe}_3\text{O}_4/\text{NaY-3.22}$ and (b) $\text{Fe}_3\text{O}_4/\text{NaY-2.55}$ at magnification of 20000. \times

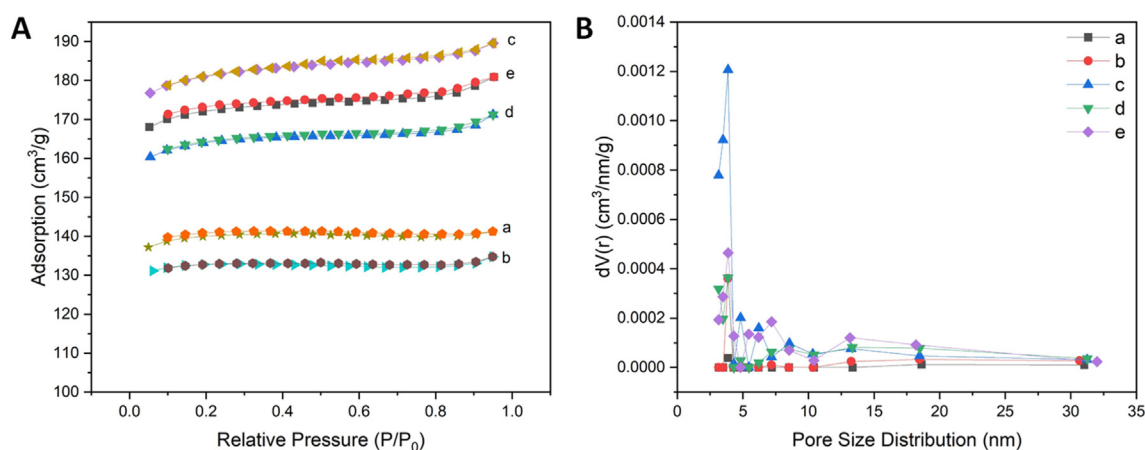


Figure 6. A. The isotherm adsorption-desorption curves and B. pore size distribution of a) NaY-Z, b) $\text{Fe}_2\text{O}_3/\text{NaY-1.7}$, c) $\text{Fe}_2\text{O}_3/\text{NaY-3.52}$, d) $\text{Fe}_3\text{O}_4/\text{NaY-2.55}$ and e) $\text{Fe}_3\text{O}_4/\text{NaY-3.22}$.

3.2. Partial oxidation of methane reaction

Figure 7 shows the experiment results in terms of the amount of total products, and selectivity towards methanol and formaldehyde. When $\text{Fe}_2\text{O}_3/\text{NaY}$ or $\text{Fe}_3\text{O}_4/\text{NaY}$ is applied, the total amount of oxygenates/weight catalyst and the selectivity towards methanol and formaldehyde are varied. Low loading of iron oxides (1.70 and 2.55 wt% of Fe) leads to the selectivity to methanol, and the total amount of oxygenates are rather similar (0.854 and 1.01 $\mu\text{mol/g}$ catalyst). Meanwhile, in the reaction using catalysts with higher loading of iron oxides ($\text{Fe}_2\text{O}_3/\text{NaY-3.52}$ and $\text{Fe}_3\text{O}_4/\text{NaY-3.22}$), the products are a mixture of methanol and formaldehyde. Using $\text{Fe}_2\text{O}_3/\text{NaY-3.52}$, formaldehyde is the dominant product (88.3% from total product of 3.872 $\mu\text{mol/g}$ catalyst); while when $\text{Fe}_3\text{O}_4/\text{NaY-3.22}$ was employed, methanol was more preferable (65.7% from 1.614 $\mu\text{mol/g}$ catalyst). As a comparison, the reaction using only Fe_3O_4 catalyst has also been conducted, giving no significant products. This indicates that Fe_3O_4 , having a magnetic character, is not a suitable catalyst for this reaction.

On the other hand, when the as-prepared NaY catalyst is used, the partial oxidation of methane produces 5.044 $\mu\text{mol/g}$ catalyst (the highest amongst the catalysts tested in this work), with the selectivity of 14.8% and 85.2% to methanol and formaldehyde, respectively. This is interesting since similar experiments using Na/ZSM-5 or H/ZSM-5 as catalysts have given no or insignificant amount of methanol.

4. Discussion

The catalytic test on partial oxidation of methane was conducted on microporous NaY zeolite and its iron-oxide modified derivatives. The

reaction adapted the reaction reported in [15] which have been explored and modified extensively using ZSM-5 zeolite as supports and several transition metal oxides active sites [16, 17, 18, 19, 37]. From previous work, it has been confirmed that for curtailed reaction time, the partial oxidation of methane gives oxygenated products although no molecular oxygen is present in the batch reactor. It is suggested that the oxides on the activated ZSM-5 surface contribute to the oxidation of methane and produce methoxy ($\text{CH}_3\text{-CO-O}$) on the surface, which required the extraction of methanol with ethanol for recovery [18]. When small amount of oxygen is introduced, the yield of products is increased, because the oxygen regenerate the used oxygen from the surface of zeolite.

When NaY is used as support for low amounts of iron-oxides, the amount of formaldehyde is suppressed, leading to the selectivity to methanol (Figure 7). This result is in agreement with the partial oxidation of methane using $\text{Fe}_2\text{O}_3/\text{hierarchical ZSM-5}$ catalyst [37], in which more methanol is produced. Figure 8a illustrates the plausible reaction mechanism of methane partial oxidation to methanol on iron-oxides/NaY. The first (step 1) starts with the diffusion of methane into iron (III) from $-\text{O-Fe-O}-$ attached to the surface of NaY. The second (step 2) is the adsorption of CH_4 on $-\text{O-Fe-O}-$, followed by (step 3) the abstraction of a hydrogen atom from CH_4 by $\alpha\text{-O}$ species to form a hydroxyl group residing on the α -site on the surface of Fe-zeolites ($\text{Fe}^{\text{III}}\text{-O-H}$ fragment) and a methyl radical $\text{CH}_3\bullet$. This $\text{CH}_3\bullet$ radical may then either react with a further $\alpha\text{-O}$ species (step 4) to produce methoxy groups $\alpha\text{-(Fe-OCH}_3\text{)}$ that may be extracted via hydrolysis or the CH_3 may be 'rebound' to form an associated ($\text{Fe}^{\text{II}}\text{-O(H)-CH}_3$). After that, $\text{CH}_3\text{-OH}$ desorbs, causing vacant oxygen which then is degenerated by O_2^- from free molecular oxygen (step 5).

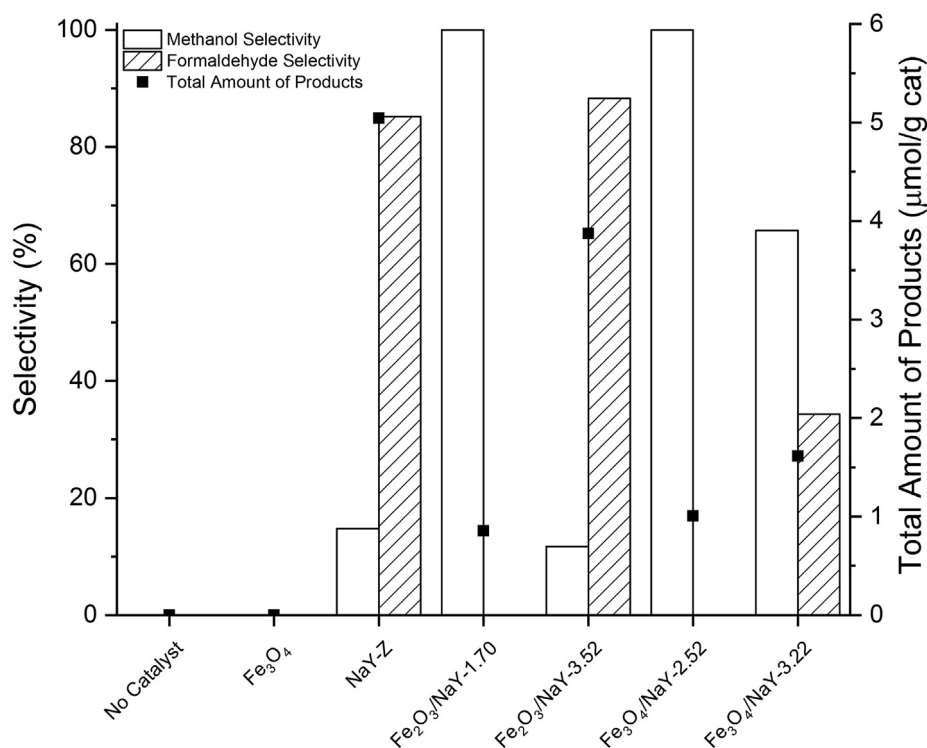


Figure 7. Selectivity towards methanol and formaldehyde and the total amount of produced oxygenates of NaY zeolites for methane partial oxidation. Reaction condition: T: 423 K, ratio N₂: O₂: CH₄ = 1.99 : 0.01: 0.75, t = 1 h.

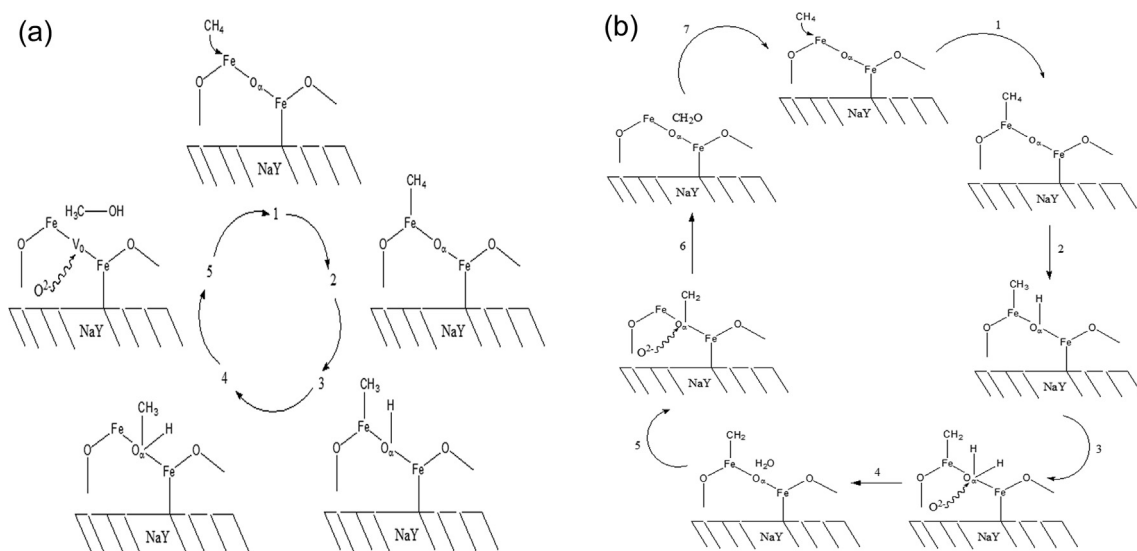


Figure 8. Plausible reaction mechanism of methane partial oxidation on Fe-oxide/NaY surface: (a) Methanol production, and (b) Formaldehyde production.

Figure 8b illustrates the suggested reaction mechanism when there is less oxygen in the iron oxides/NaY. The 1–3 steps are similar to the mechanism in Figure 8a followed by another abstraction of a hydrogen atom to produce H–O–H (step 4). The H–O–H then desorbs H₂O leaving vacant oxygen (step 5). The O² from free molecular oxygen then replaces the vacant oxygen (step 6). In step 7, the CH₂• radical reacts with the α-O species and desorbs as CH₂O (formaldehyde) and the vacant oxygen is regenerated. These tentative reaction mechanisms are suggested based on the explanation by Cheng *et al* [38] for methane oxidation.

The type of zeolite framework used as catalyst support shows that it plays an important role in the reaction. The Si/Al ratio of NaY is lower than that of ZSM-5, which makes it more acidic (has more Lewis acidic

sites). Furthermore, NaY has a more homogeneous pore shape and size (all microporous) and higher surface area, compared to the previously studied ZSM-5 [16]. The first step of methane conversion over metal-oxides/zeolite is the activation of the C–H bond of methane into radical C–H (Figure 8). Raynes *et al* [39] and Arzumanov *et al* [40] explained that Lewis acidic sites promote methane activation by forming a sigma complex prior to the C–H bond cleavage. The C–H bond of methane, which is more electron-rich, favors the coordination over the C–H bond of methanol, which is relatively electron-poor.

In contrast, when thermally activated NaY-Z zeolite is an active catalyst for partial oxidation of methane and giving the highest amount of products and selectivity to formaldehyde. Figure 9a suggests the

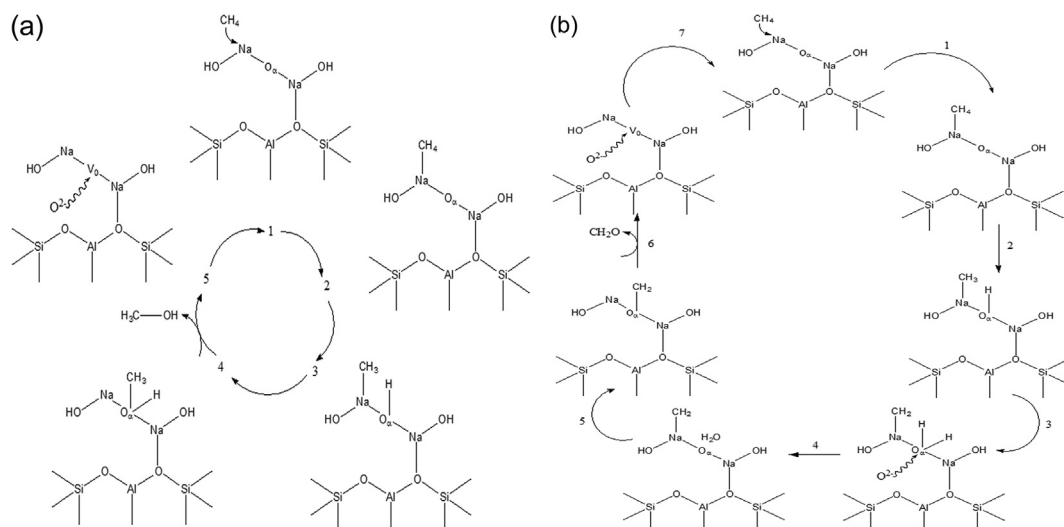


Figure 9. Plausible reaction mechanism of methane partial oxidation on NaY-Z surface: (a) Methanol production, and (b) Formaldehyde production.

mechanism reaction of methane partial oxidation to methanol on NaY. The low Si/Al ratio of NaY-Z (4.20) should contribute to this reactivity, in which the $-\text{O}-\text{Na}-\text{O}-$ extra framework could interact with methane. Since Y zeolite has more acidic Lewis site (Al sites where the Na^+ ions reside) than ZSM-5, it is suggested that more coordination of the C-H bond of methane to the $-\text{Na}-\text{O}-$ extra framework takes place and experiences further oxidation to formaldehyde (Figure 9b). Thus, in this work, by using NaY-Z as catalyst, the reaction is more selective to the production of formaldehyde. This is in agreement with work reported by Bitter et.al, that acid-treated Co/ZSM-5 has selectivity to formaldehyde than to methanol [15]. More work should be done to investigate the reactivity of NaY zeolite.

5. Conclusion

Partial oxidation of methane, in the presence of two type of iron oxide-modified NaY zeolites, has been carried out in mild conditions. The reaction shows that the as-synthesized NaY zeolite is a good catalyst to produce formaldehyde, while the presence of Fe_2O_3 or Fe_3O_4 impregnated on the NaY surfaces results in a selectivity to methanol. The presence of NaY zeolite as support is shown to be crucial because the reaction with Fe_3O_4 without support shows no catalytic activity for this reaction.

Declarations

Author contribution statement

Yuni Krisyuningsih Krisnandi: Conceived and designed the experiments; Analyzed and interpreted the data; Contributed reagents, materials, analysis tools or data; Wrote the paper.

Dita Arifa Nurani: Conceived and designed the experiments; Wrote the paper.

Dheo Vany Alfian: Performed the experiments; Analyzed and interpreted the data; Wrote the paper.

Uwin Sofyani: Performed the experiments; Analyzed and interpreted the data.

Muhammad Faisal: Performed the experiments.

Indah Revita Saragi: Analyzed and interpreted the data; Wrote the paper.

Afif Zulfikar Pamungkas: Analyzed and interpreted the data; Wrote the paper.

Arnia Putri Pratama: Analyzed and interpreted the data; Wrote the paper.

Funding statement

This work was supported by Universitas Indonesia (NKB-1949/UN2.R3.1/HKP.05.00/2019).

Data availability statement

Data included in article/supplementary material/referenced in article.

Declaration of interests statement

The authors declare no conflict of interest.

Additional information

Supplementary content related to this article has been published online at <https://doi.org/10.1016/j.heliyon.2021.e08305>.

Acknowledgements

The authors would like to thank Universitas Indonesia for funding this research through Universitas Indonesia Collaboration Research Grant with contract number NKB-1949/UN2.R3.1/HKP.05.00/2019. Professor Russell Howe is greatly acknowledged for early discussion in partial oxidation of methane over zeolite catalyst. Mr. R. A. Rafsanjani is thanked for the XRD and XRF measurement.

References

- [1] B.F. Cai, et al., Estimation of methane emissions from municipal solid waste landfills in China based on point emission sources, *Adv. Clim. Change Res.* 5 (2) (Jan. 2014) 81–91.
- [2] D. Díaz-Vázquez, S.C. Alvarado-Cummings, D. Meza-Rodríguez, C. Senés-Guerrero, J. de Anda, M.S. Gradilla-Hernández, Evaluation of biogas potential from livestock manures and multicriteria site selection for centralized anaerobic digester systems: the case of Jalisco, Mexico, *Sustain.* 12 (9) (2020).
- [3] M.C. Alvarez-Galvan, N. Mota, M. Ojeda, S. Rojas, R.M. Navarro, J.L.G. Fierro, Direct methane conversion routes to chemicals and fuels, *Catal. Today* 171 (1) (Aug. 2011) 15–23.
- [4] G. Senthamaraiakannan, D. Chakrabarti, V. Prasad, Transport fuel-LNG and methane, in: *Future Energy: Improved, Sustainable and Clean Options for Our Planet*, 2013, pp. 271–288.
- [5] H. Schwarz, *Chemistry with Methane: Concepts rather than Recipes*, *Angewandte Chemie - International Edition*, 2011.
- [6] B. Wang, S. Albarracín-Suazo, Y. Pagán-Torres, E. Nikolla, Advances in methane conversion processes, *Catal. Today* 285 (2017) 147–158.

- [7] R. Horn, R. Schlögl, Methane activation by heterogeneous catalysis, *Catal. Lett.* 145 (2015) 23–39.
- [8] M. Ravi, M. Ranocchiari, J.A. van Bokhoven, The Direct Catalytic Oxidation of Methane to Methanol—A Critical Assessment, *Angewandte Chemie - International Edition*, 2017, pp. 16464–16483.
- [9] P. Schwach, X. Pan, X. Bao, Direct conversion of methane to value-added chemicals over heterogeneous catalysts: challenges and prospects, *Chem. Rev.* (2017) 8497–8520.
- [10] A.I. Olivos-Suarez, Á. Szécsényi, E.J.M. Hensen, J. Ruiz-Martinez, E.A. Pidko, J. Gascon, Strategies for the direct catalytic valorization of methane using heterogeneous catalysis: challenges and opportunities, *ACS Catal.* 6 (5) (May 2016) 2965–2981.
- [11] R. Sharma, H. Poelman, G.B. Marin, V.V. Galvita, Approaches for selective oxidation of methane to methanol, *Catalysts* 10 (2) (Feb. 01, 2020) 194. MDPI AG.
- [12] A. Rosa, G. Ricciardi, E.J. Baerends, Is $[\text{FeO}]^{2+}$ the active center also in iron containing zeolites? A density functional theory study of methane hydroxylation catalysis by Fe-ZSM-5 zeolite, *Inorg. Chem.* (2010).
- [13] E.V. Starokon, M.V. Parfenov, L.V. Pirutko, S.I. Abornev, G.I. Panov, Room-temperature oxidation of methane by α -oxygen and extraction of products from the FeZSM-5 surface, *J. Phys. Chem. C* (2011).
- [14] E.V. Starokon, M.V. Parfenov, S.S. Arzumanov, L.V. Pirutko, A.G. Stepanov, G.I. Panov, Oxidation of methane to methanol on the surface of FeZSM-5 zeolite, *J. Catal.* 300 (2013) 47–54.
- [15] N.V. Beznis, A.N.C. Van Laak, B.M. Weckhuysen, J.H. Bitter, Oxidation of methane to methanol and formaldehyde over Co-ZSM-5 molecular sieves: tuning the reactivity and selectivity by alkaline and acid treatments of the zeolite ZSM-5 agglomerates, *Microporous Mesoporous Mater.* 138 (1–3) (Feb. 2011) 176–183.
- [16] Y.K. Krisnandi, B.A.P. Putra, M. Bahtiar, Zahara, I. Abdullah, R.F. Howe, Partial oxidation of methane to methanol over heterogeneous catalyst Co/ZSM-5, *Procedia Chem.* (2015).
- [17] Y.K. Krisnandi, B.A. Samodro, R. Sihombing, R.F. Howe, Direct synthesis of methanol by partial oxidation of methane with oxygen over cobalt modified mesoporous H-ZSM-5 catalyst, *Indones. J. Chem.* 15 (3) (2015) 263–268.
- [18] Y.K. Krisnandi, et al., “Partial Oxidation of Methane to Methanol on Cobalt Oxide-Modified Hierarchical ZSM-5,” in *Biogas [Working Title]*, IntechOpen, 2019.
- [19] B.G. Nurgita, D.A. Nurani, Y.K. Krisnandi, Partial oxidation of methane to methanol over MxOy/ZSM-5 (Mn, Fe, Co, and Ni) hierarchical transition metal oxide catalysts, in: *IOP Conference Series: Materials Science and Engineering* 496, Feb. 2019, p. 1.
- [20] D.A. Nurani, Y.K. Krisnandi, A. Akmal, Partial Oxidation of Methane over NiOx/Hierarchical ZSM-5 Catalyst, 2018.
- [21] E.B.G. Johnson, S.E. Arshad, Hydrothermally synthesized zeolites based on kaolinite: a review, *Appl. Clay Sci.* 97 (98) (2014) 215–221.
- [22] Z. Liu, C. Shi, D. Wu, S. He, B. Ren, A simple method of preparation of high silica zeolite y and its performance in the catalytic cracking of cumene, *J. Nanotechnol.* 2016 (2016).
- [23] Y.F. Shen, J. Tang, Z.H. Nie, Y.D. Wang, Y. Ren, L. Zuo, Preparation and application of magnetic Fe₃O₄ nanoparticles for wastewater purification, *Separ. Purif. Technol.* (2009).
- [24] M.M.J. Treacy, J.B. Higgins, *Collection of Simulated XRD Powder Patterns for Zeolites Fifth (5th) Revised Edition*, 2007.
- [25] R. Rt, A.-A. Sd, K. Hh, M. Hs, Preparation and Characterization of Hematite Iron Oxide (α -Fe₂O₃) by Sol-Gel Method, 2018.
- [26] W. Wang, L. Zheng, F. Lu, R. Hong, M.Z.Q. Chen, L. Zhuang, Facile synthesis and characterization of magnetochromatic Fe₃O₄ nanoparticles, *AIP Adv.* 7 (5) (2017) 1–8.
- [27] W.A. Khanday, S.A. Majid, S. Chandra Shekar, R. Tomar, Synthesis and characterization of various zeolites and study of dynamic adsorption of dimethyl methyl phosphate over them, *Mater. Res. Bull.* (2013).
- [28] A.P. Pratama, D.U.C. Rahayu, Y.K. Krisnandi, Levulinic acid production from delignified rice husk waste over manganese catalysts: Heterogeneous versus homogeneous, *Catalysts* (2020).
- [29] S. Guru, D. Mishra, M. Singh, S.S. Amritphale, S. Joshi, Effect of SO₄²⁻, Cl⁻ and NO₃⁻ anions on the formation of iron oxide nanoparticles via microwave synthesis, *Protect. Met. Phys. Chem. Surface* 52 (4) (Jul. 2016) 627–631.
- [30] I. Revita Saragi, Y. Krisyuningsih Krisnandi, R. Sihombing, Synthesis and characterization HY zeolite from natural aluminosilicate for n-hexadecane cracking, *Mater. Today Proc.* 13 (2019) 76–81.
- [31] Y.K. Krisnandi, et al., Synthesis and characterization of crystalline NaY-zeolite from belitung kaolin as catalyst for n-hexadecane cracking, *Crystals* 9 (8) (2019) 404.
- [32] A.A. Dabbawala, et al., Synthesis of hierarchical porous Zeolite-Y for enhanced CO₂ capture, *Microporous Mesoporous Mater.* (2020).
- [33] M. Naderi, *Surface Area : Brunauer – Emmett – Teller (BET)*, 2015, pp. 585–608.
- [34] K. El-Boubbou, et al., Preparation of iron oxide mesoporous magnetic microparticles as novel multidrug carriers for synergistic anticancer therapy and deep tumor penetration, *Sci. Rep.* 9 (1) (Dec. 2019) 11481.
- [35] S.E.E. Misi, A. Ramli, F.H. Rahman, Characterization of the structure feature of bimetallic Fe-Ni catalysts, *J. Appl. Sci.* 11 (7) (2011) 1297–1302.
- [36] Y. Wang, Q. Zhang, T. Shishido, K. Takehira, Characterizations of iron-containing MCM-41 and its catalytic properties in epoxidation of styrene with hydrogen peroxide, *J. Catal.* 209 (1) (2002) 186–196.
- [37] A.T. Putrananda, D.A. Nurani, Y.K. Krisnandi, Synthesis of metal oxide-hierarchical ZSM-5 (CO₃O₄/ZSM-5 and Fe₂O₃/ZSM-5) as catalysts for partial oxidation of biomethane to methanol, in: *IOP Conference Series: Materials Science and Engineering* 763, Apr. 2020, p. 12029, no. 1.
- [38] Z. Cheng, L. Qin, J.A. Fan, L.S. Fan, New insight into the development of oxygen carrier materials for chemical looping systems, *Engineering* 4 (3) (2018) 343–351.
- [39] S. Raynes, M.A. Shah, R.A. Taylor, Direct conversion of methane to methanol with zeolites: towards understanding the role of extra-framework d-block metal and zeolite framework type, *Dalton Trans.* 48 (28) (2019) 10364–10384.
- [40] S. S. Arzumanov, A. A. Gabrienko, D. Freude, and A. G. Stepanov, “Competitive pathways of methane activation on Zn²⁺-modified ZSM-5 zeolite: H/D hydrogen exchange with Brønsted acid sites: versus dissociative adsorption to form Zn-methyl species,” *Catal. Sci. Technol.*, vol. 6, no. 16, pp. 6381–6388.